

# Simulation and modeling of BEGe detectors

Matteo Agostini, Calin A. Ur,

E. Bellotti, D. Budjáš, C. Cattadori, A. di Vacri, A. Garfagnini, L. Pandola, S. Schönert

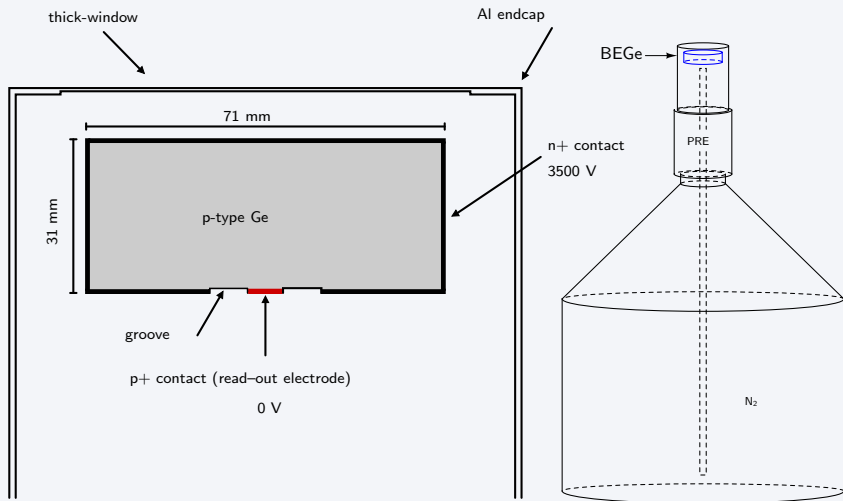
Max-Planck-Institute für Kernphysik

MaGe meeting, January 18th 2010



- 1 The BEGe detectors
- 2 The simulation
  - The structure of the simulation
  - Design and implementation of the simulation
- 3 Validation of the simulation
  - Validation of the MaGe simulation
  - Validation of the PSS
- 4 Conclusion

## The BEGe geometry



## The (LNGS) BEGe features

**Electrical Characteristics:**

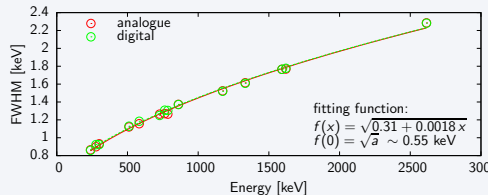
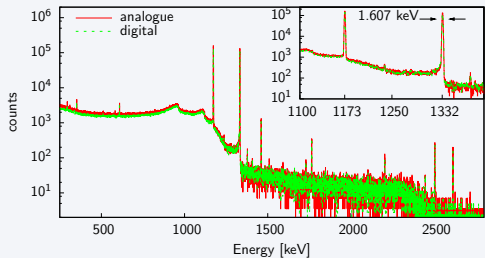
Depletion voltage	+3000 V
Operational bias voltage	+3500 V
Integral nonlinearity	< 0.05%

**Physical Characteristics:**

Active diameter	71 mm
Active area	3800 mm <sup>2</sup>
Thickness	32 mm
Distance from window	5 mm
Efficiency	> 34%

**Energy Resolution at 1332.5 keV:**

FWHM (nominal)	1.752 keV
FWHM (measured)	1.607 ± 0.003 keV
FWTM	3.259 keV



# The structure of the simulation

## I. MC simulation

- > coordinates and energy of the hits

## II. Signal formation and development

- <- coordinate of each hit
- > electron and hole trajectories
- > the signal induced on the point size electrode

## III. DAQ simulations

- <- energy and signal for each hit in an event
- <- the Preamplifier Transfer Function (PTF)
- > each pulse is convolved with the PTF
- > all the pulses of an event are added up
- > the noise is added to the total pulse

# The structure of the simulation

## I. MC simulation

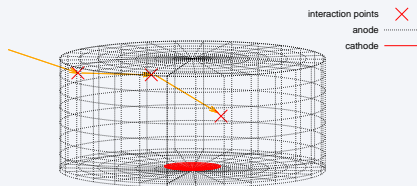
-> coordinates and energy of the hits

## II. Signal formation and development

- <- coordinate of each hit
- > electron and hole trajectories
- > the signal induced on the point size electrode

## III. DAQ simulations

- <- energy and signal for each hit in an event
- <- the Preamplifier Transfer Function (PTF)
- > each pulse is convolved with the PTF
- > all the pulses of an event are added up
- > the noise is added to the total pulse



# The structure of the simulation

## I. MC simulation

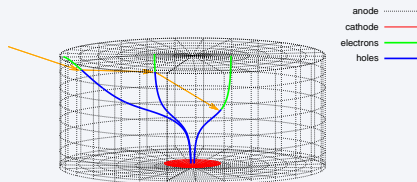
- > coordinates and energy of the hits

## II. Signal formation and development

- <- coordinate of each hit
- > electron and hole trajectories
- > the signal induced on the point size electrode

## III. DAQ simulations

- <- energy and signal for each hit in an event
- <- the Preamplifier Transfer Function (PTF)
- > each pulse is convolved with the PTF
- > all the pulses of an event are added up
- > the noise is added to the total pulse



# The structure of the simulation

## I. MC simulation

→ coordinates and energy of the hits

## II. Signal formation and development

← coordinate of each hit

→ electron and hole trajectories

→ the signal induced on the point size electrode

## III. DAQ simulations

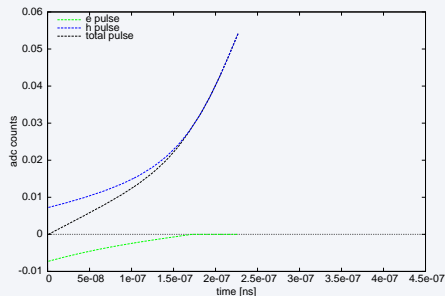
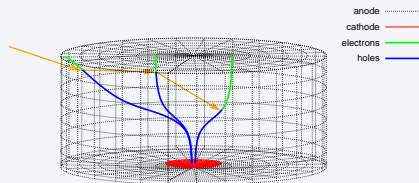
← energy and signal for each hit in an event

← the Preamplifier Transfer Function (PTF)

→ each pulse is convolved with the PTF

→ all the pulses of an event are added up

→ the noise is added to the total pulse





# The structure of the simulation

## I. MC simulation

→ coordinates and energy of the hits

## II. Signal formation and development

← coordinate of each hit

→ electron and hole trajectories

→ the signal induced on the point size electrode

## III. DAQ simulations

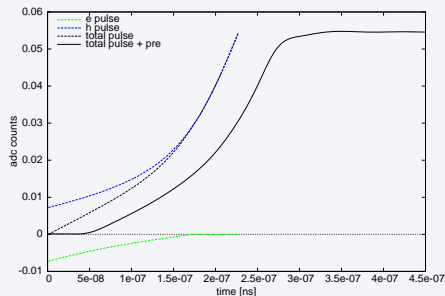
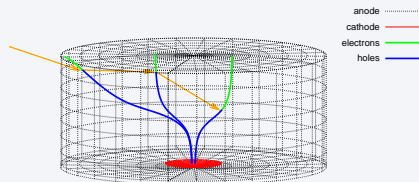
← energy and signal for each hit in an event

← the Preamplifier Transfer Function (PTF)

→ each pulse is convolved with the PTF

→ all the pulses of an event are added up

→ the noise is added to the total pulse



# The structure of the simulation

## I. MC simulation

→ coordinates and energy of the hits

## II. Signal formation and development

← coordinate of each hit

→ electron and hole trajectories

→ the signal induced on the point size electrode

## III. DAQ simulations

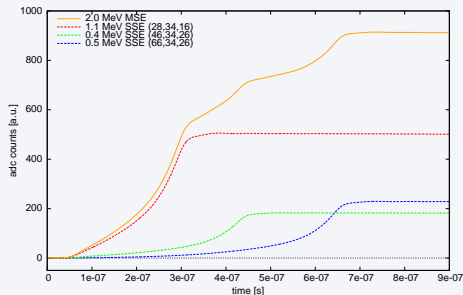
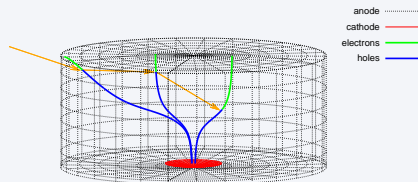
← energy and signal for each hit in an event

← the Preamplifier Transfer Function (PTF)

→ each pulse is convolved with the PTF

→ all the pulses of an event are added up

→ the noise is added to the total pulse



# The structure of the simulation

## I. MC simulation

→ coordinates and energy of the hits

## II. Signal formation and development

← coordinate of each hit

→ electron and hole trajectories

→ the signal induced on the point size electrode

## III. DAQ simulations

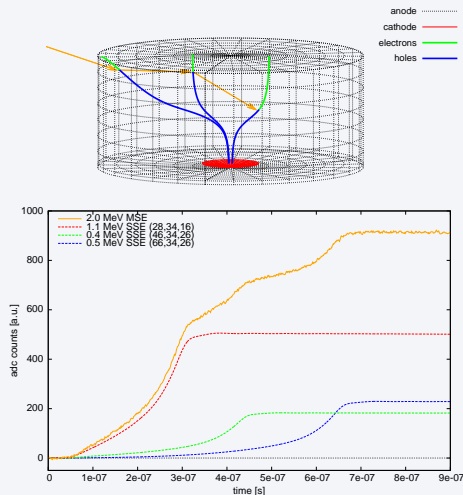
← energy and signal for each hit in an event

← the Preamplifier Transfer Function (PTF)

→ each pulse is convolved with the PTF

→ all the pulses of an event are added up

→ the noise is added to the total pulse



# The simulation design

step 0. Create a library of pulses:

- 0.1 divide the detector in cubic cell ( $1 \text{ mm} \times 1 \text{ mm} \times 1 \text{ mm}$ )  
and generate a pulse for each cell
- 0.2 convolve each pulse with the PTF
- 0.3 store all the pulses in a library

step 1. Run the MC simulation

step 2. For each hit compute the pulse as weighted average of the pulses stored in the library

step 3. For each event compute the total pulse by adding up the pulse of each hit

step 4. Add the noise

# The simulation design

step 0. Create a library of pulses:

- 0.1 divide the detector in cubic cell ( $1 \text{ mm} \times 1 \text{ mm} \times 1 \text{ mm}$ )  
and generate a pulse for each cell
- 0.2 convolve each pulse with the PTF
- 0.3 store all the pulses in a library

← MGS

step 1. Run the MC simulation

step 2. For each hit compute the pulse as weighted average of the pulses stored in the library

step 3. For each event compute the total pulse by adding up the pulse of each hit

step 4. Add the noise

MGS v 5r02 : Multi Geometry Simulation is a MATLAB software developed for the AGATA project (<http://www.iphc.cnrs.fr/-MGS-.html> )

# The simulation design

step 0. Create a library of pulses:

0.1 divide the detector in cubic cell ( $1 \text{ mm} \times 1 \text{ mm} \times 1 \text{ mm}$ )

and generate a pulse for each cell

<- MGS

0.2 convolve each pulse with the PTF

0.3 store all the pulses in a library

step 1. Run the MC simulation

<- MaGe

step 2. For each hit compute the pulse as weighted average of the pulses stored in the library

step 3. For each event compute the total pulse by adding up the pulse of each hit

step 4. Add the noise

MGS v 5r02 : Multi Geometry Simulation is a MATLAB software developed for the AGATA project (<http://www.iphc.cnrs.fr/-MGS-.html> )

MaGe: BEGe geometry used `munichteststand/GELNGSBEGeDetector.hh`

## MGS: simulation of the signal formation and development

## Trajectory simulation

Fourth-order Runge-Kutta method ( $\Delta t = 1$  ns):

$$\mathbf{r}(t + \Delta t) = \mathbf{r}(t) + f(\mathbf{v}(\mathbf{r}(t)), \Delta t)$$

where the velocity is computed by using the mobility model of L. Mihailescu and B. Bruynell:

$$\mathbf{v}_h = \mu_h(\mathbf{r}, \mathbf{E}) \cdot \mathbf{E} \quad \mathbf{v}_e = \mu_e(\mathbf{r}, \mathbf{E}) \cdot \mathbf{E}$$

## Simulation of the Electric Field

SOR and relaxation method to solve the Poisson's eq:

$$\nabla^2 \phi(\mathbf{r}) = -\frac{\rho(\mathbf{r})}{\epsilon} \rightarrow \mathbf{E}(\mathbf{r}) = -\nabla(\phi(\mathbf{r}))$$

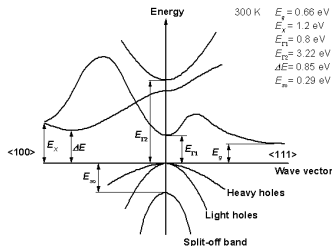
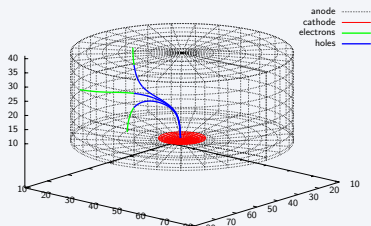
- cathode at 0 V, anode at 3500 V
- detector completely depleted:  $\rho(\mathbf{r}) = eN_A(\mathbf{r})$

## Signal computation

Shockley-Ramo Theorem:

$$Q(t) = -q\phi_w(\mathbf{r}(t))$$

where  $\phi_w(\mathbf{r}(t))$  is the weighting potential



## MGS: simulation of the signal formation and development

## Trajectory simulation

Fourth-order Runge-Kutta method ( $\Delta t = 1 \text{ ns}$ ):

$$\mathbf{r}(t + \Delta t) = \mathbf{r}(t) + f(\mathbf{v}(\mathbf{r}(t)), \Delta t)$$

where the velocity is computed by using the mobility model of L. Mihailescu and B. Bruynell:

$$\mathbf{v}_h = \mu_h(\mathbf{r}, \mathbf{E}) \cdot \mathbf{E} \quad \mathbf{v}_e = \mu_e(\mathbf{r}, \mathbf{E}) \cdot \mathbf{E}$$

## Simulation of the Electric Field

SOR and relaxation method to solve the Poisson's eq:

$$\nabla^2 \phi(\mathbf{r}) = -\frac{\rho(\mathbf{r})}{\epsilon} \rightarrow \mathbf{E}(\mathbf{r}) = -\nabla(\phi(\mathbf{r}))$$

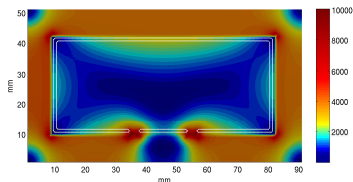
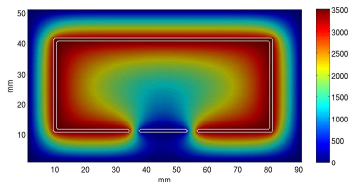
- cathode at 0 V, anode at 3500 V
- detector completely depleted:  $\rho(\mathbf{r}) = eN_A(\mathbf{r})$

## Signal computation

Shockley-Ramo Theorem:

$$Q(t) = -q\phi_w(\mathbf{r}(t))$$

where  $\phi_w(\mathbf{r}(t))$  is the weighting potential





## MGS: simulation of the signal formation and development

## Trajectory simulation

Fourth-order Runge-Kutta method ( $\Delta t = 1 \text{ ns}$ ):

$$\mathbf{r}(t + \Delta t) = \mathbf{r}(t) + f(\mathbf{v}(\mathbf{r}(t)), \Delta t)$$

where the velocity is computed by using the mobility model of L. Mihailescu and B. Bruynell:

$$\mathbf{v}_h = \mu_h(\mathbf{r}, \mathbf{E}) \cdot \mathbf{E} \quad \mathbf{v}_e = \mu_e(\mathbf{r}, \mathbf{E}) \cdot \mathbf{E}$$

## Simulation of the Electric Field

SOR and relaxation method to solve the Poisson's eq:

$$\nabla^2 \phi(\mathbf{r}) = -\frac{\rho(\mathbf{r})}{\epsilon} \rightarrow \mathbf{E}(\mathbf{r}) = -\nabla(\phi(\mathbf{r}))$$

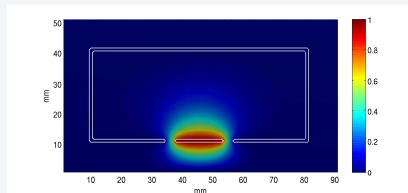
- cathode at 0 V, anode at 3500 V
- detector completely depleted:  $\rho(\mathbf{r}) = eN_A(\mathbf{r})$

## Signal computation

Shockley-Ramo Theorem:

$$Q(t) = -q\phi_w(\mathbf{r}(t))$$

where  $\phi_w(\mathbf{r}(t))$  is the weighting potential

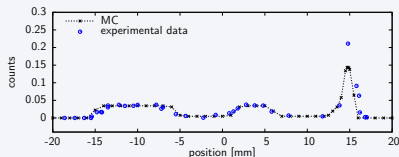
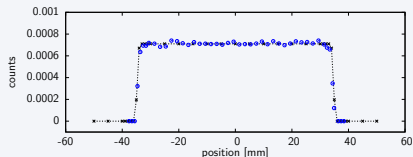


The *weighting potential* is defined as the electric potential calculated when the considered electrode is kept at a unit potential, all other electrodes are grounded and all charges inside the device are removed.

## Validation of the MaGe simulation

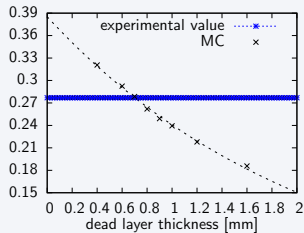
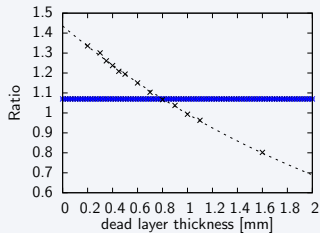
→ Housing absorption

scanning with a collimated source of Am along a diameter and the side:



→ Dead layer measurements (nominal dead layer 0.8 mm)

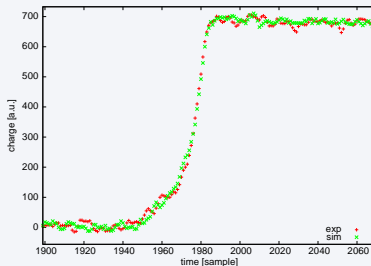
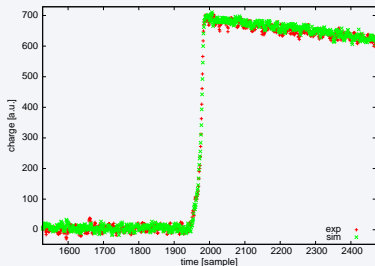
ratio between the counts in the peaks at 81 keV and at 356 keV of  $^{133}\text{Ba}$ :



# Validation of the PSS

The validation was carried out by comparing directly the simulated and the experimental signals:

- $^{241}\text{Am}$  colimated source  $\Rightarrow$  well localized events close to the detector surface;
- averaging up the experimental and simulated signals  $\Rightarrow$  reduction of noise



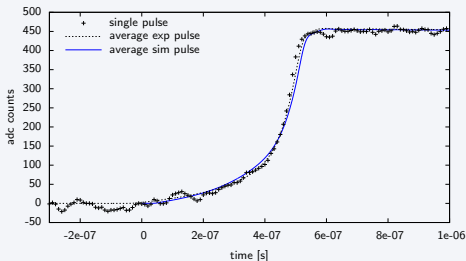
# Validation of the PSS

The validation was carried out by comparing directly the simulated and the experimental signals:

- $^{241}\text{Am}$  colimated source  $\Rightarrow$  well localized events close to the detector surface;
- averaging up the experimental and simulated signals  $\Rightarrow$  reduction of noise

## The averaging algorithm steps:

- 1 the experimental signal (sampled at 10 ns) is resampled at 1 ns interpolating the original points with the FADC transfer function;
- 2 the resampled signal is fitted with the average in order to obtain the best possible time alignment;
- 3 if the average rms is minor than the threshold value, the resampled and shifted signal is accepted in the average.

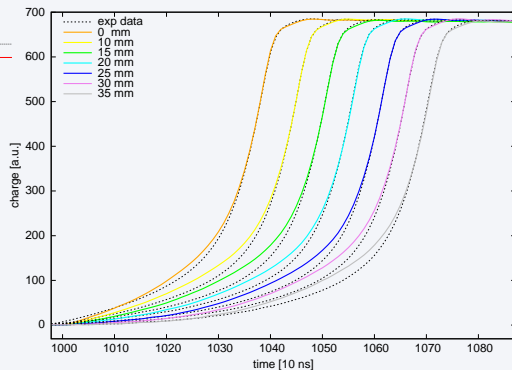
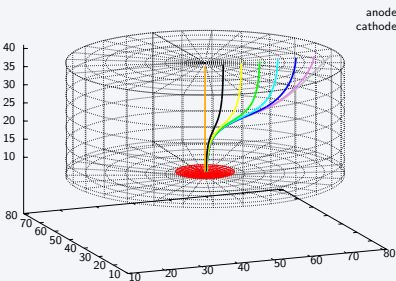


## Radial scanning

->  $^{241}\text{Am}$  source

-&gt; 2 mm collimator

-&gt; 600 s acquisitions for each position



The holes are dragged to the center of the detector and then drift to the p+ contact with a common trajectory

⇒ pulse shape discrimination parameter  $A/E^a$  depends on the final rising part only which is largely independent of the position of interaction inside crystal

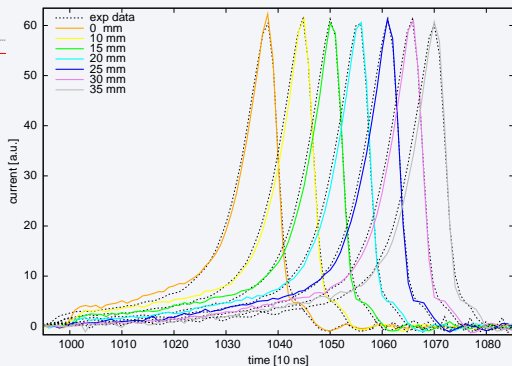
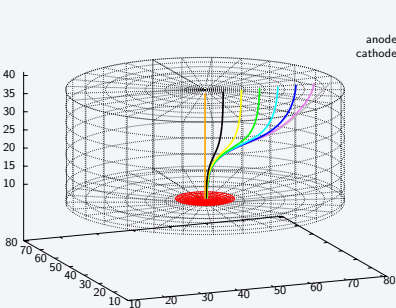
$^a A \rightarrow$  max amplitude of the current pulse;  $E \rightarrow$  total energy of the event

## Radial scanning

->  $^{241}\text{Am}$  source

-&gt; 2 mm collimator

-&gt; 600 s acquisitions for each position



The holes are dragged to the center of the detector and then drift to the  $p^+$  contact with a common trajectory

⇒ pulse shape discrimination parameter  $A/E^a$  depends on the final rising part only which is largely independent of the position of interaction inside crystal

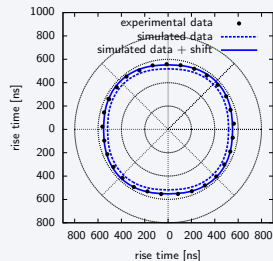
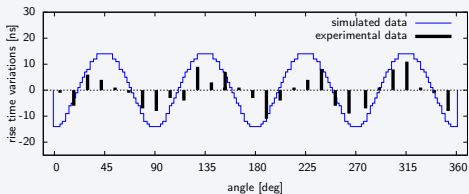
$^a A \rightarrow$  max amplitude of the current pulse;  $E \rightarrow$  total energy of the event

## Circular Scanning

->  $^{241}\text{Am}$  source      -> 1 mm collimator      -> 500 s acquisitions for each position

We study the rise time as a function of the angle.

-> To observe variations we used the rise time between 1% and 90%



Although the experimental data show a behaviour coherent with the simulation, the agreement is only qualitative.

⇒ the result is remarkable taking into account the problems related to the identification of the time corresponding to the 1% of the maximum amplitude

# Conclusion

## Results:

- the simulations performed with the nominal geometry is in reasonable quantitative agreement with the experimental data
- the impact of detector parameters (i.e. geometry description, grid step, impurity distribution, bias voltage, etc.) on the signal pulse shape has been studied and the simulation accuracy could be improved.



# Conclusion

## Results:

- the simulations performed with the nominal geometry is in reasonable quantitative agreement with the experimental data
- the impact of detector parameters (i.e. geometry description, grid step, impurity distribution, bias voltage, etc.) on the signal pulse shape has been studied and the simulation accuracy could be improved.

## Future works:

- investigate the pulse shape discrimination performances of BEGe detectors by using simulations:
  - compare PS discrimination performance of experimental data with the simulation
  - study the impact of the detector parameters on pulse shape discrimination performances and the robustness of A/E method
  - determine the depletion voltage and the best operational voltage
- validate the simulation with a precise inner scanning of the detector
- generate library for the Phase I detectors and study PSA detector

# Conclusion

## Results:

- the simulations performed with the nominal geometry is in reasonable quantitative agreement with the experimental data
- the impact of detector parameters (i.e. geometry description, grid step, impurity distribution, bias voltage, etc.) on the signal pulse shape has been studied and the simulation accuracy could be improved.

## Future works:

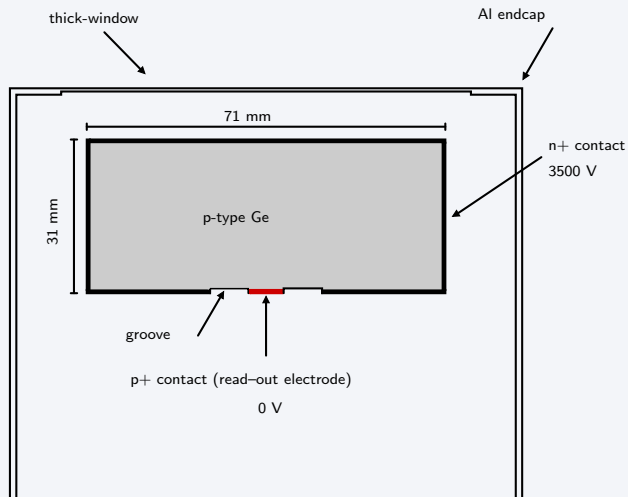
- investigate the pulse shape discrimination performances of BEGe detectors by using simulations:
  - compare PS discrimination performance of experimental data with the simulation
  - study the impact of the detector parameters on pulse shape discrimination performances and the robustness of A/E method
  - determine the depletion voltage and the best operational voltage
- validate the simulation with a precise inner scanning of the detector
- generate library for the Phase I detectors and study PSA detector

-> We are writing a paper containing these results (March-April)

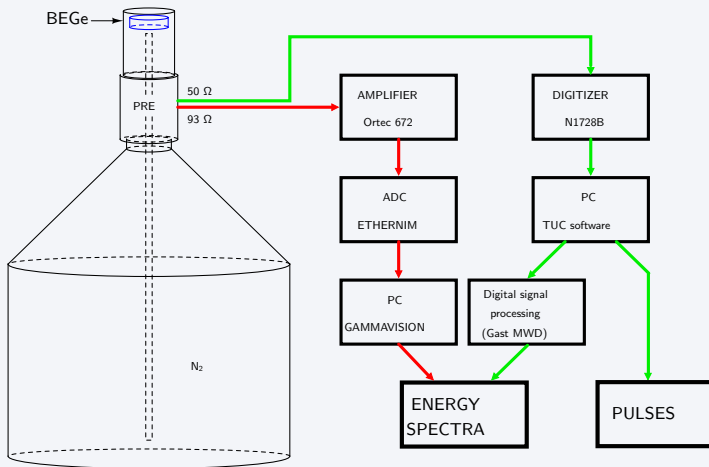
-> The beta version of the simulation software will be soon uploaded to the MaGe repository.

backup slides

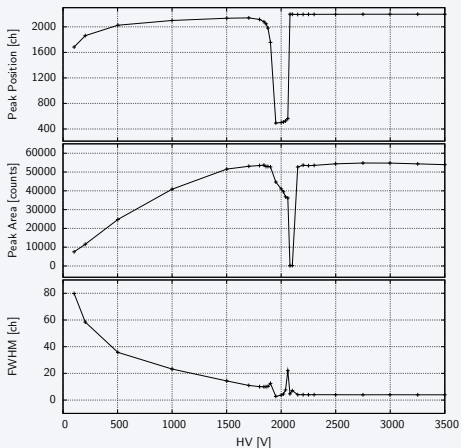
## BEGe detector



## DAQ systems



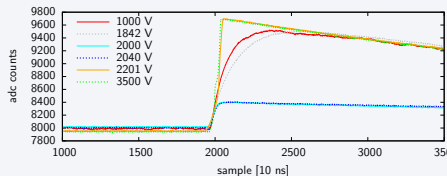
## HV scanning



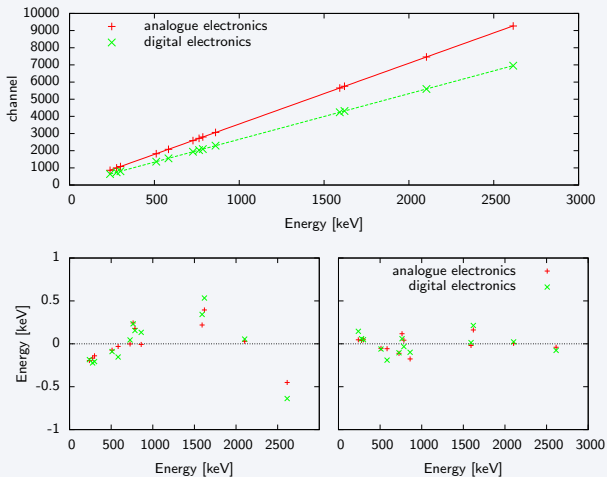
*region I [2045 V, 3500 V]:*  
 excellent performances, detector full depleted,  
 rise time  $\sim 0.5\mu\text{s}$ , amplitude  $\sim 0.3\text{ V}$ .

*region II [1860 V, 2045 V]:*  
 anomalous behaviour, pulses still fast but their  
 amplitudes four times smaller.

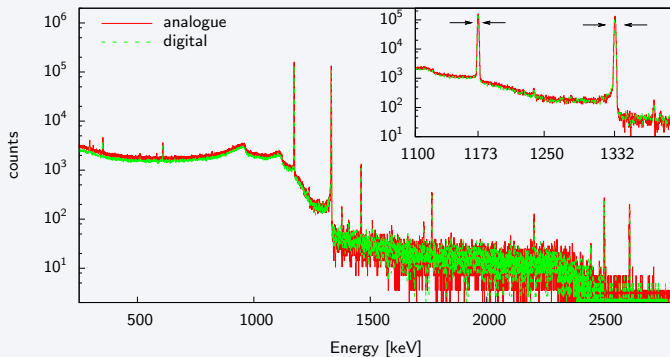
*region III [100 V, 1860 V]:*  
 detector partially depleted, charge collection not  
 complete, detector capacitance increment, slower  
 rise time  $\sim 5\mu\text{s}$ .



# Characterization measurements - Linearity



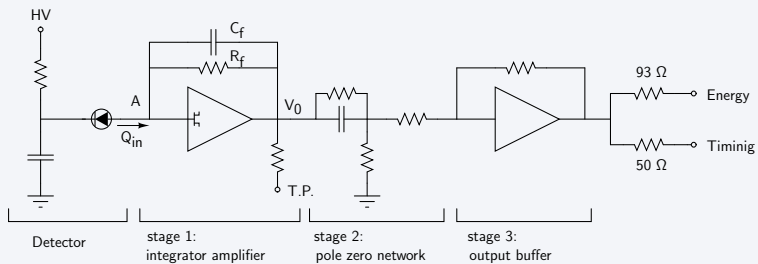
# Characterization measurements - Resolution



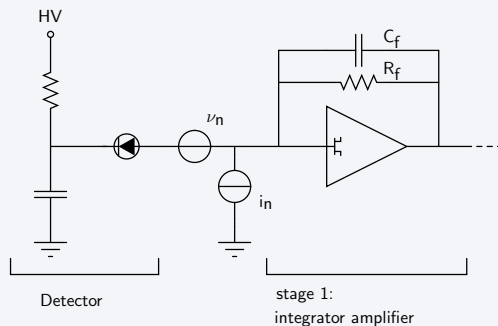
Energy [keV]	Analogue DAQ system		Digital DAQ system	
	peak counts	FWHM [keV]	peak counts	FWHM [keV]
1173	259899 (510)	1.529 (0.002)	224857 (506)	1.520 (0.002)
1332	225023 (474)	1.617 (0.002)	200137 (518)	1.607 (0.003)



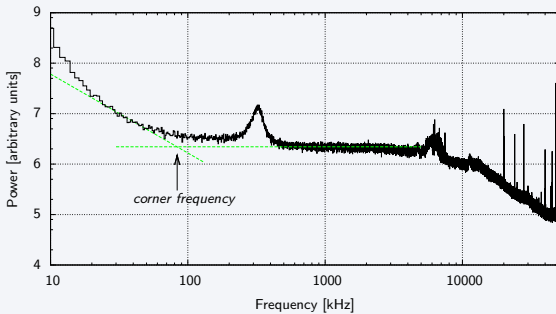
# Characterization measurements - Preamplifier



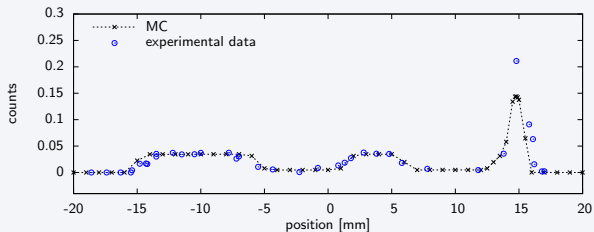
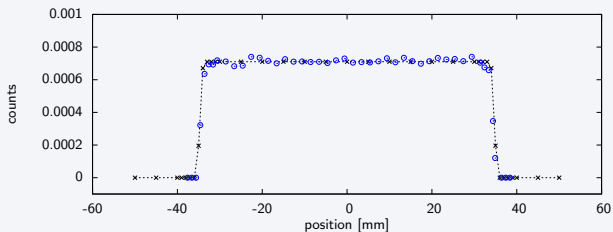
## Characterization measurements - Preamplifier noise



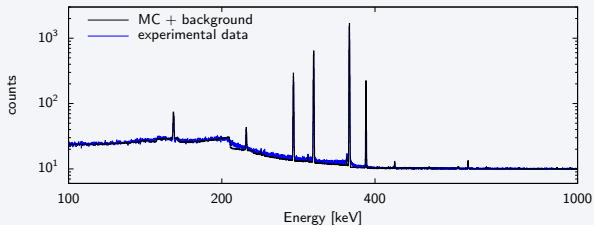
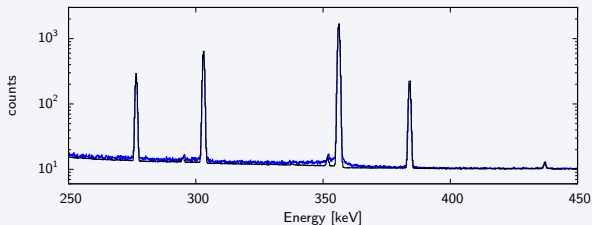
## Characterization measurements - Preamplifier noise



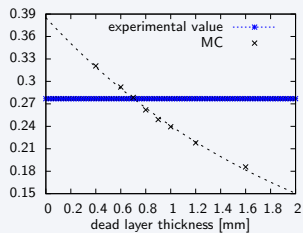
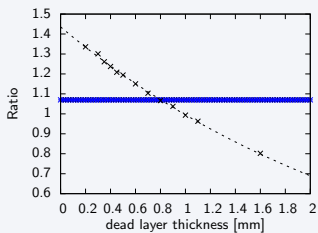
## Validation of the MAGE simulation - Absorption



## Validation of the MAGE simulation - Barium spectrum



## Validation of the MAGE simulation - DL



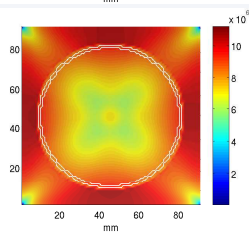
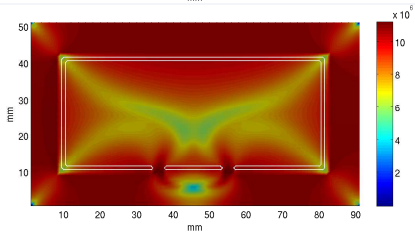
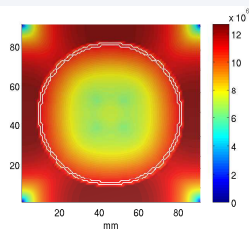
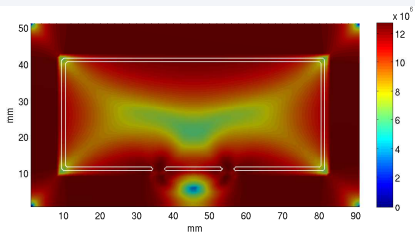
## Mobility model

$$\mathbf{v}_{exp} = \frac{\mu_0 \mathbf{E}}{(1 + (\mathbf{E}/\mathbf{E}_0)^\beta)^{1/\beta}} - \mu_n \mathbf{E}$$

$$\mathbf{v}_d = \mathcal{A}(|\mathbf{E}|, T) \sum_j \frac{n_j}{n} \frac{\gamma_j \mathbf{E}_0}{(\mathbf{E}_0 \gamma_j \mathbf{E}_0)^{1/2}}$$

$$\mathbf{v}_d \approx \begin{pmatrix} v_r \\ v_\theta \\ v_\phi \end{pmatrix} = \mathbf{v}_{100}(E) \begin{pmatrix} 1 - \Lambda(k_0) \sin^4(\theta_0) \sin^2(2\phi_0) + \sin^2(2\theta_0) \\ \Omega(k_0) [2 \sin^3(\theta_0) \cos(\theta_0) \sin^2(2\phi_0) + \sin(4\theta_0)] \\ \Omega(k_0) \sin^3(\theta_0) \sin(4\phi_0) \end{pmatrix}$$

## Drift velocity





# How to compute the electric field in a semiconductor detector

Since a semiconductor detector can be considered as an electrostatic system, the electric field can be computed by solving the following Maxwell's equations or, equivalently, by solving the **Poisson's equation**:

$$\left. \begin{aligned} \nabla \cdot \mathbf{E} &= \frac{\rho}{\varepsilon} \\ \nabla \times \mathbf{E} &= 0 \Rightarrow \mathbf{E} = -\nabla\phi \end{aligned} \right\} \nabla \cdot \nabla\phi = -\frac{\rho}{\varepsilon} \Rightarrow \nabla^2\phi = -\frac{\rho}{\varepsilon}$$

To solve the Poisson's equation  $\nabla^2\phi = -\rho/\varepsilon$  and find the potential  $\phi$  we need to know:

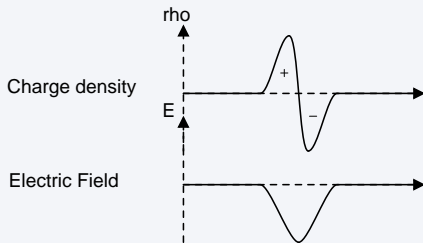
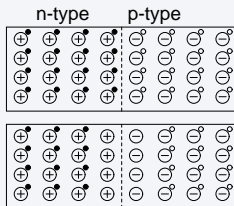
- the charge density distribution  $\rho$
- the boundary conditions (the value of  $\phi$  on some surfaces):

$$\phi_0|_{S_{cathode}} = V_{cathode} \text{ and } \phi_0|_{S_{anode}} = V_{anode}$$

# The semiconductor junction

The semiconductor detector functioning is based on the properties of a semiconductor junction:

- holes
- ⊖ Acceptor ions
- electrons
- ⊕ Donor ions



The junction formation:

I. Spontaneous diffusion  $e \rightarrow \leftarrow h$

because of the difference in the concentration of electrons and holes between the two materials, there is an initial diffusion of the holes towards the n-region and a similar diffusion of electrons towards the p-region

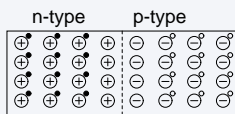
II. Recombination  $e \bullet \rightarrow \leftarrow \bullet h$

the diffusing electrons fill up holes in the p-region while the diffusing holes capture electrons in the n-side

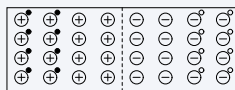
III. Thermodynamic equilibrium  $\leftarrow \bullet e \xrightarrow{E} \leftarrow \oplus \quad \ominus \rightarrow h \bullet$

the recombination creates a net charge distribution inside the semiconductor. This creates an electric field gradient across the junction which halts the diffusion process.

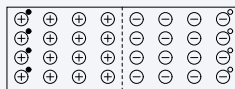
# The charge distribution dependence of an external electric field



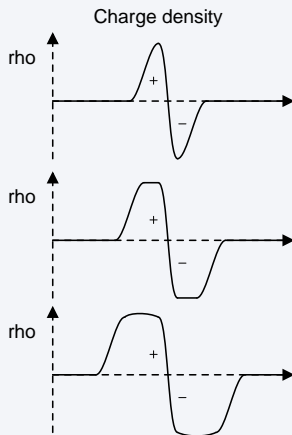
$E_{ext} = 0$



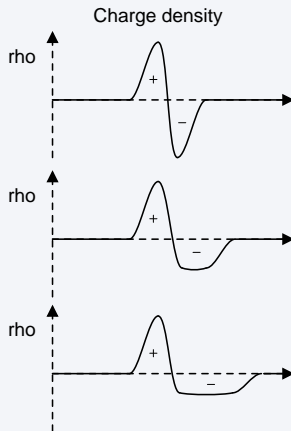
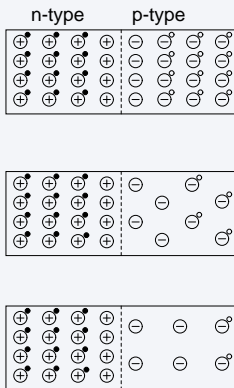
$E_{ext}$



$E_{ext}$

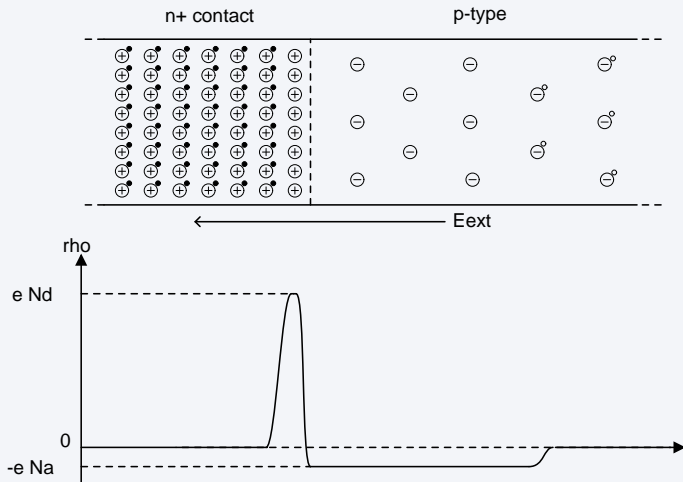


# The charge distribution dependence of the impurity concentrations



# The charge distribution in a real detector

In a real semiconductor the junction is created between an heavily doped semiconductor and a high-purity semiconductor:



# The assumptions

In all the potential computation we will assume that:

- the detector is fully depleted  
p-type detector  $\Rightarrow \rho = -eN_d$   
n-type detector  $\Rightarrow \rho = eN_a$
- the boundary conditions are:  
the voltage on the electrodes is defined by the HV supply  
 $\Rightarrow \phi|_{cathode} = 0 \text{ V}$   
 $\Rightarrow \phi|_{anode} = 3000 \text{ V}$   
the detector is enclosed in a vacuum chamber  
 $\Rightarrow \phi|_{ext} = 0 \text{ V}$

# The linear superposition principle – the potential

From the linear superposition principle the potential can be separated into two contribution:

$$\phi(\mathbf{r}) = \phi_0(\mathbf{r}) + \phi_\rho(\mathbf{r})$$

where:

- $\phi_0$  is the potential calculated considering only the electrode potentials ( $\rho(\mathbf{r}) = 0 \quad \forall \mathbf{r}$ )
- $\phi_\rho$  is the potential obtained grounding all the electrodes

The linearity of the Maxwell's equation allows for computing the Poisson's equation for each contribution and then add up all the contribution:

$$\nabla^2 \phi_0(\mathbf{r}) = 0 \quad \text{with: } \phi_0|_{S_{cathode}} = V_{cathode} \quad \phi_0|_{S_{anode}} = V_{anode}$$

$$\nabla^2 \phi_\rho(\mathbf{r}) = -\rho(\mathbf{r})/\varepsilon \quad \text{with: } \phi_\rho|_{S_{cathode}} = 0 \quad \phi_\rho|_{S_{anode}} = 0$$

where  $S_{anode}$  and  $S_{cathode}$  are the boundary surface of the two electrodes.

## The linear superposition principle – the field

Similarly, since the electric field is determined by the *linear* relation  $\mathbf{E} = -\nabla\phi$ , it can be divided into two components:

$$\mathbf{E}(\mathbf{r}) = \mathbf{E}_0(\mathbf{r}) + \mathbf{E}_\rho(\mathbf{r})$$

where:

- $\mathbf{E}_0(\mathbf{r}) = -\nabla\phi_0(\mathbf{r})$
- $\mathbf{E}_\rho(\mathbf{r}) = -\nabla\phi_\rho(\mathbf{r})$



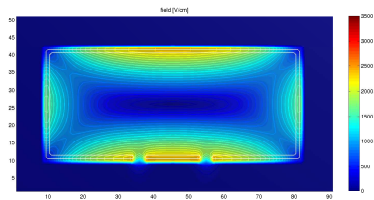
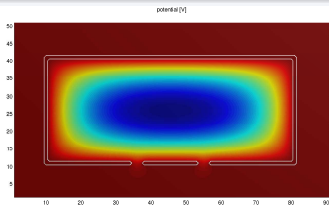
# How to solve the Poisson's equation

The Poisson's equation is solved analytically only in the simplest problem, usually it is solved by using numerical methods. In our simulation we use two algorithms which works on a grid:

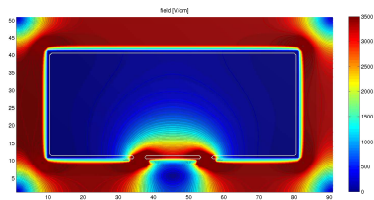
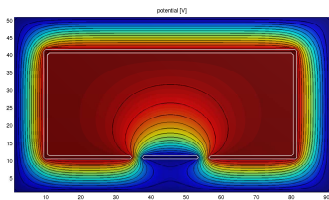
- **The Successive Over Relaxation (SOR) method** converges to a solution replacing at each iteration the current approximated solution at a given grid point by a weighted average of its nearest neighbour on the grid
- **the relaxation method** converges by replacing at each iteration the current approximated solution with its Taylor expansion computed for each point on the grid.

## Comparison

$$\phi_\rho$$

$$E_\rho$$


$$\phi_0$$

$$E_0$$


$$\phi_{tot}$$

$$E_{tot}$$
